1 # Supporting Information for
2 Functionality of potato virus Y coat protein in cell-to-cell movement
3 dynamics is defined by its N terminal region

4 Anže Vozelj[1,2*], Tjaša Mahkovec Povalej[1], Katja Stare[1], Magda Tušek Žnidarič[1], Katarina Bačnik[1],
5 Valentina Levak[1,2], Ion Gutiérrez-Aguirre[1], Marjetka Podobnik[3], Kristina Gruden[1], Anna Coll[1]†,
6 Tjaša Lukan[1]†*

7 * Corresponding authors. Email: anze.vozelj@nib.si, tjasa.lukan@nib.si

8 **This PDF file includes:**
9
10 **Supplementary Text S1.** Construction of PVY-N605(123)- GFP CP N-terminal mutants
11 **Fig. S1.** ΔN50-CP ΔN40-CP viral replication.
12 **Fig. S2.** Viral replication ΔN26-CP.
13 **Fig. S3.** ΔN19-CP_ΔN14-CP_WT-CP cell-to-cell spread dynamics.
14 **Fig. S4.** ΔN26-CP inability of systemic spread
15 **Fig. S5.** Independent experiment for point mutants G20P, P24A and WT-CP to check
16 viral abundance.
17 **Fig. S6.** Cell-to-cell viral spread of D14A, E18A, G20P, S21G and P24A point mutants.
18 **Fig. S7.** Virus abundance D14A, E18A, WT-CP.
19 **Fig. S8.** Point mutants systemic spread.
20 **Fig. S9.** Alignment of first 50 amino acid residues from the PVY N terminal region across
21 all PVY isolates.
22 **Fig. S10.** Transmission electron microscopy (TEM) micrographs of deletion and point
23 mutants.
24 **Table S1.** ΔN26-CP viral limitation on single cells or cell-to-cell spread.
25 **Table S2.** Replication efficiency of ΔN40-CP and S21G mutant is the same as the one of
26 WT-CP PVY.
27
28 **Other supporting materials for this manuscript are openly available on Zenodo**
29 **(https://doi.org/10.5281/zenodo.17643798), including the following:**
30
31 **Dataset S1 (Microsoft Excel format).** Normalized qPCR data for constructed PVY
32 mutants.
33 **Dataset S2 (Microsoft Excel format).** General sample information including sample
34 name, plant and leaf number, date of putting plants into the soil, date of bombardment.
35 **Dataset S3 (Microsoft Excel format).** Viral cell-to-cell spread evaluation after *N.*
36 *clevelandii* inoculation with constructed mutant ΔN23/G-CP and WT-CP.
37 **Dataset S4 (Microsoft Excel format).** Viral cell-to-cell spread evaluation after *N.*
38 *clevelandii* inoculation with constructed mutants ΔN19-CP, ΔN14-CP and WT-CP.
39 **Dataset S5 (Microsoft Excel format).** Viral cell-to-cell spread evaluation after *N.*
40 *clevelandii* inoculation with constructed mutants ΔN19-CP, ΔN14-CP and WT-CP in
41 replicate experiment.
42 **Dataset S6 (Microsoft Excel format).** Foci analysis comparisons between experiments.
43 **Dataset S7 (Microsoft Excel format).** Systemic spread dynamic analysis.
44 **Dataset S8 (Microsoft Excel format).** Systemic viral spread of G20P and P24A point
45 mutants.
46 **Dataset S9 (Microsoft Excel format).** Systemic viral spread of G20P and P24A point
47 mutants in replicate experiment.
48 **Dataset S10 (Microsoft Excel format).** Systemic viral spread of D14A point mutant.
49 **Dataset S11 (Microsoft Excel format).** Systemic viral spread of E18A point mutant.
50 **Dataset S12 (Microsoft Excel format).** Primers and megaprimers sequences.

51 **Supporting Information Text S1. Construction of PVY-N605(123)- GFP CP N-terminal**
52 **mutants.**

53 Mutants were prepared with mutagenic PCR using QuikChange II XL Site-Directed Mutagenesis
54 Kit (Agilent Technologies). As a template previously constructed GFP infectious clone PVY-
55 N605(123) was used (1). The megaprimers were synthesized using the N-terminal region
56 sequence of GFP tagged PVY-N605(123) plasmid, according to defined guidelines (2). All
57 megaprimers used in the study are listed in dataset S12. Mutagenic touchdown PCR reaction
58 program with the following reaction mixture in the final volume of 25 μL were the same for all
59 generated mutants according to previously published protocol for generation of PVY deletion
60 mutants (2), with minor modifications listed below.

Component	**Final concentration**	**Volume [μL]**
10x reaction buffer	1x	2,5
dNTP mix	200 μM	0,5
forward megaprimer	0,5 μM	1,25
reverse megaprimer	0,5 μM	1,25
QuikSolution	/	1,5
PVY-N605(123)	200 ng	1,2
PfuUltra HF DNA polymerase	/	1

61

Temperature	Time	Step
92ºC	2 min	hold
92ºC	50 s	
65ºC to 55ºC	50 s	10cycles
68ºC	30 min*	
92ºC	50 s	
55ºC	50 s	8 cycles
68ºC	30 min*	
68ºC	60 min	hold

62

63

64 After amplification, 4 μL of DpnI enzyme (Agilent Technologies) was added to the mutagenesis
65 reaction mixture, following 2h on 37ºC incubation. Following DpnI digestion, 2 μL of mutagenesis
66 mixture was used for transformation into *E. coli* XL-10 Gold Ultracompetent Cells (Agilent
67 Technologies). We used 45 μL cell aliquot supplemented with 2 μL of β-mercaptoethanol for the
68 standard heat-shock transformation protocol in accordance with the manufacturer's instructions
69 (Agilent Technologies). Transformation mixtures were plated on LB agar containing ampicillin and
70 incubated overnight at 37ºC. Transformants were analyzed with colony PCR using primers PVY
71 GFP_F and PVY uni_R with KAPA2G Robust HotStart Kit (Agilent Technologies) with the
72 following 10 μL reaction mixture and cycling conditions stated below.

73

74

Component	Final concentration	Volume [µL]
5x Buffer B	1x	2
10 mM dNTP	200 µM	0,2
10 µM PVY GFP_F	300 nM	0,3
10 µM PVY uni_R	300 nM	0,3
5 U/µL KAPA2G polymerase	0,3 U	0,06
Colony suspension	/	1
H20		6,14

Temperature	Time	Step
95 °C	10min	Hold
95 °C	30 s	
55 °C	15 s	30 cycles
72 °C	1 min	
72 °C	5 min	Hold

75 Sanger sequencing, using the same primers as for the colony PCR, of positive colonies was
76 performed to confirm correct sequence of the PVY coding part.
77

78 Designed mutants PVY-N605(123)-GFP with desired mutations were amplified in One Shot®

79 TOP10 *E. coli* and 50 μg of constructed plasmid mutants were isolated from overnight cultures

80 using GenElute Plasmid MiniPrep Kit (Sigma-Aldrich). Isolated plasmids were subsequently used

81 to coat 6.25 mg of gold microcarriers (0,6 μm) to prepare gene gun bullets according to the

82 manufacturers protocol and were used for *Nicotiana clevelandii* bombardment using a

83 Helios®gene gun (Bio-Rad) at 200 psi (2).

84

85 **Supporting figures and tables**

86

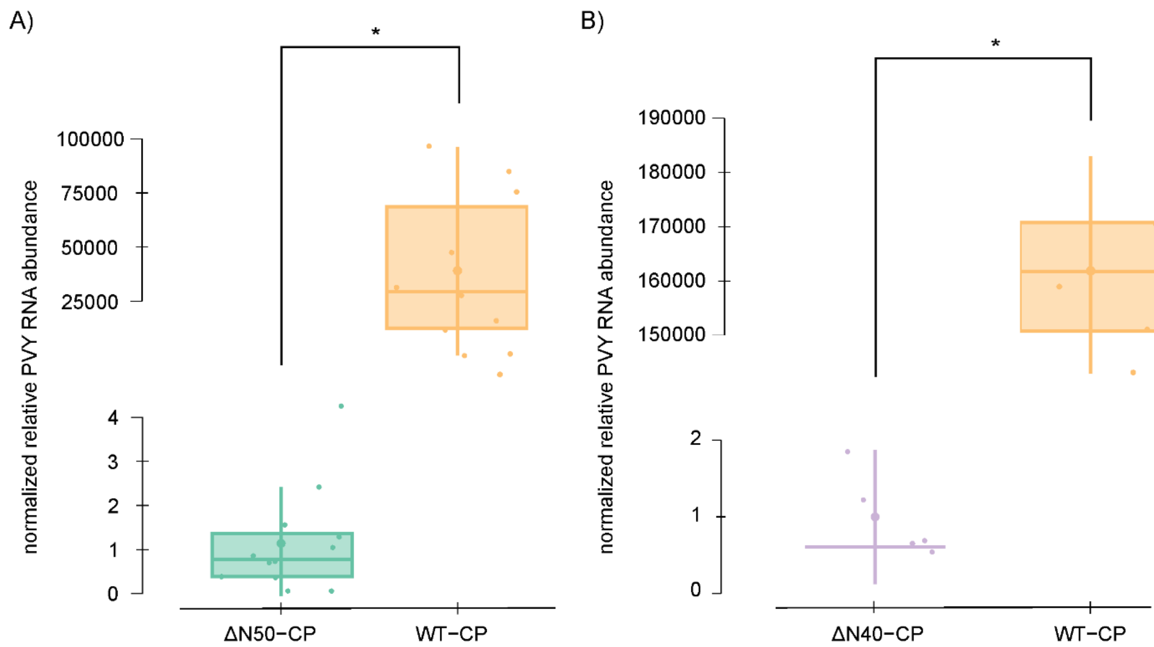

87
88

89 **Fig. S1. ΔN50-CP ΔN40-CP viral replication**. Normalized relative PVY RNA abundance in
90 bombarded *N. clevelandii* leaves for constructed PVY mutants lacking 50 (ΔN50-CP) (A) and 40
91 (ΔN40-CP) (B) amino acids at CP N-terminus. Results were obtained 14 days post bombardment
92 (dpb). Non-mutated infectious clone (WT-CP) was used as a control. Data normalization was
93 performed as described in dataset S1. Results are presented as boxplots with normalized relative
94 PVY RNA abundance for each sample shown as dots. Differences between ΔN50-CP and WT-CP
95 and between ΔN50-CP and WT-CP were statistically evaluated using Welch's t test. Statistically
96 significant differences (p<0,05) are marked with an asterisk (*). Vertical lines present all points
97 except outliers.

98

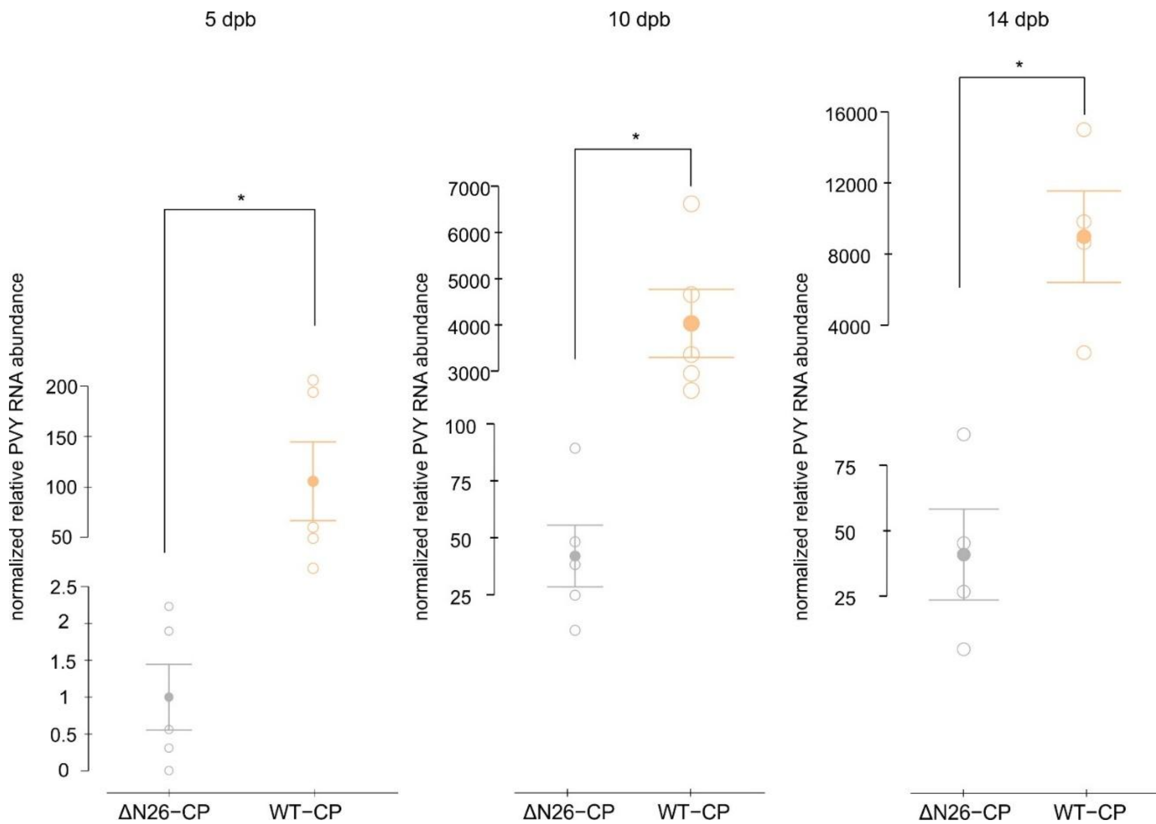

99
100

101 **Fig. S2. Viral replication ΔN26-CP.** Normalized relative PVY RNA abundance in bombarded *N.*
102 *clevelandii* leaves for constructed PVY mutant lacking 26 amino acids residues, in three
103 timepoints including 5, 10 and 14 dpb (from left to right). Non-mutated infectious clone (WT-CP)
104 was used as a control. Data normalization was performed as described in dataset S1. Results are
105 presented as mean (represented with filled dot) and standard error. Individual measurements are
106 shown as empty dots, representing normalized relative PVY RNA abundance. Differences
107 between constructed deletion mutants and WT-CP were statistically evaluated using Welch's t
108 test. Statistically significant differences (p<0,05) are marked with an asterisk (*). Note that the
109 scales are different between time points.

110

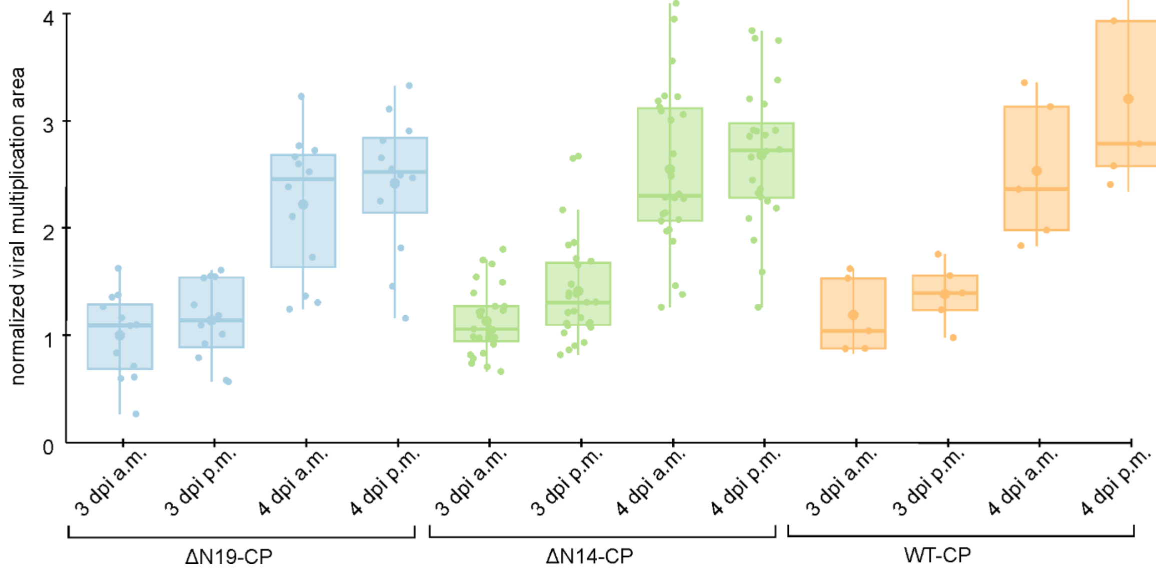

111

112 **Fig. S3. N19-CP_ΔN14-CP_WT-CP cell-to-cell spread dynamics.** Viral cell-to-cell spread
113 dynamics was quantified with normalized viral multiplication analysis as described in Materials
114 and methods. Results are presented as boxplots for tested mutants ΔN19-CP, ΔN14-CP and WT-
115 CP in 4 tested timepoints including 3 dpi a.m., 3 dpi p.m., 4 dpi a.m. and 4 dpi p.m., where dots
116 are representing normalized viral multiplication area as described in dataset S5. Differences
117 were statistically evaluated using Welch`s t test. Vertical lines present all points except outliers.
118 The differences were not statistically significant, due to autofluorescence of trichomes which
119 resulted in saturated pixels.

120

121
122

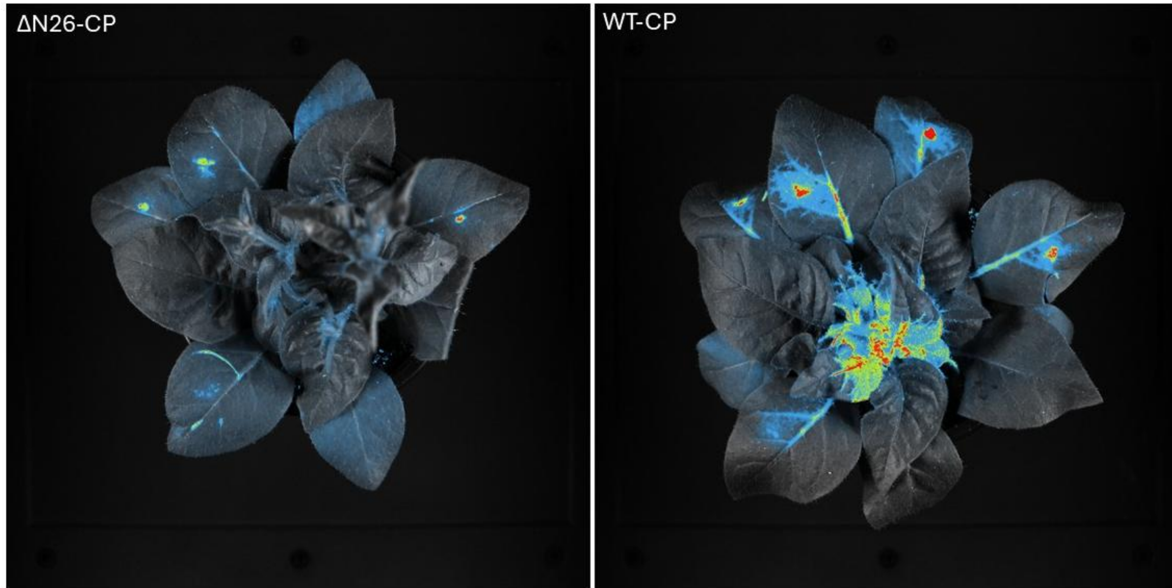

123 **Fig. S4. ΔN26-CP inability of systemic spread.** Viral systemic spread was abolished in ΔN26-

124 CP mutant (left) in comparison to non mutated WT-CP, where systemic spread occurred (right).

125 Pictures taken 12 dpb.

126

127

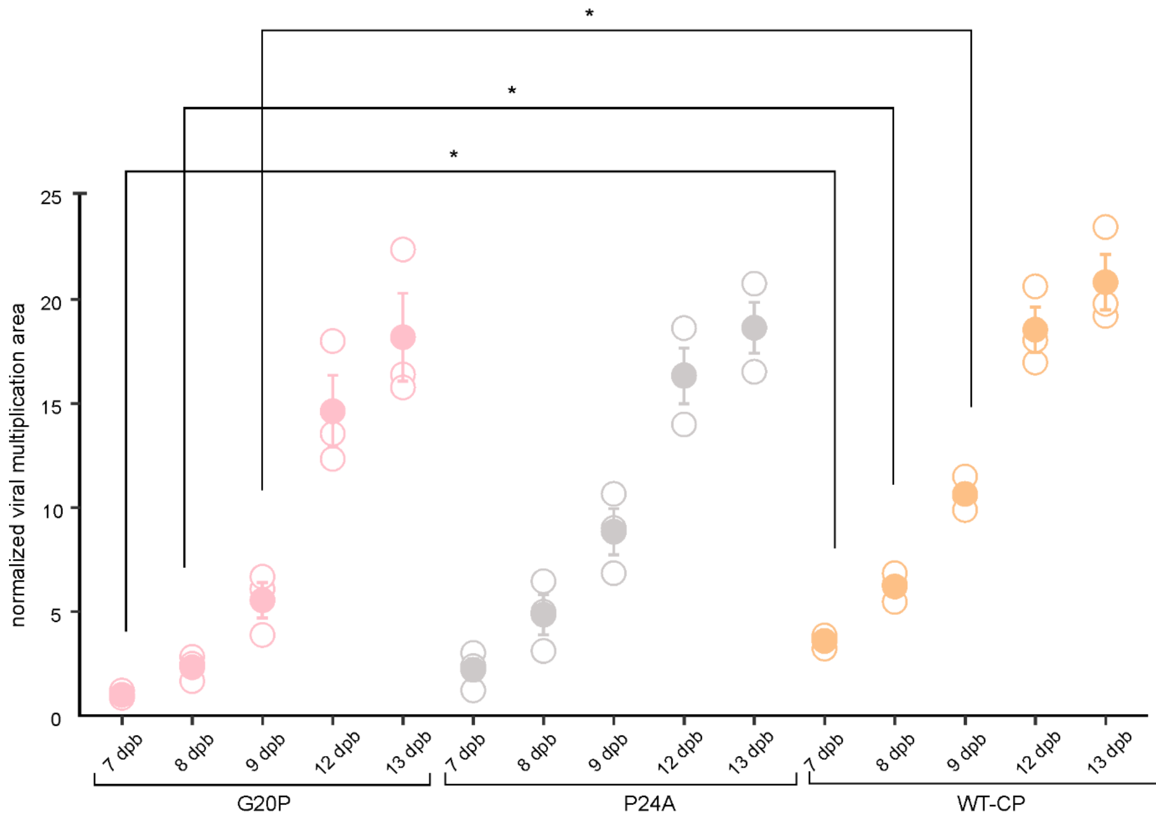

128

129 **Fig. S5. Independent experiment for point mutants G20P, P24A and WT-CP to check viral**
130 **abundance.** Quantification of virus abundance in the upper leaves of bombarded *N. clevelandii*
131 expressed as total count per mutant 7, 8, 9, 12 and 13 dpb with exposure time 50 s (A). Other
132 measurements settings are the same as stated in Materials and methods. Mean (represented
133 with filled dot) and standard error are shown. Individual measurements are shown as empty dots,
134 representing normalized viral multiplication area. Statistically significant difference in normalized
135 viral multiplication area between mutants was evaluated by Welch`s t test. Statistically significant
136 differences (p<0,05) are demarked with an asterisk (*). Raw and normalized data, number of
137 plants and results of statistical analysis are specified in dataset S9. Note that there was no
138 statistically significant difference between G20P and WT-CP at 12 and 13 dpb due to signal
139 oversaturation due to high exposure time (50 s).

140

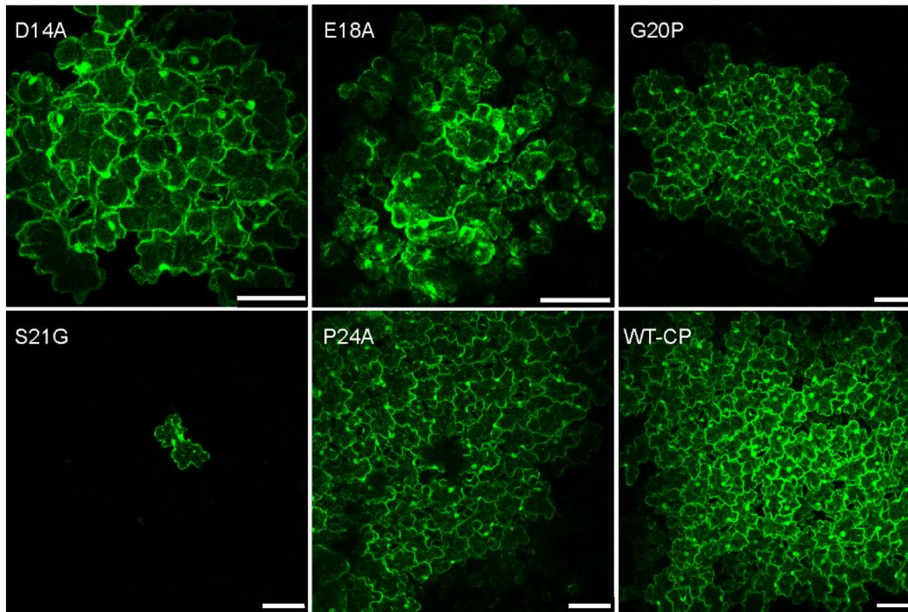

141 **Fig. S6. Cell-to-cell viral spread of D14A, E18A, G20P, S21G and P24A point mutants.**

142 Confocal microscopy images showing viral cell-to-cell spread of D14A, E18A, G20P, S21G, P24A

143 point mutants and WT-CP 5 dpb. Note that there we have comparisons of D14A and E18A point

144 mutants with the others (G20P, S21G, P24A) already included in the article main text (Fig. 4B).

145 Other confocal microscopy settings are specified in Materials and methods.

146

147

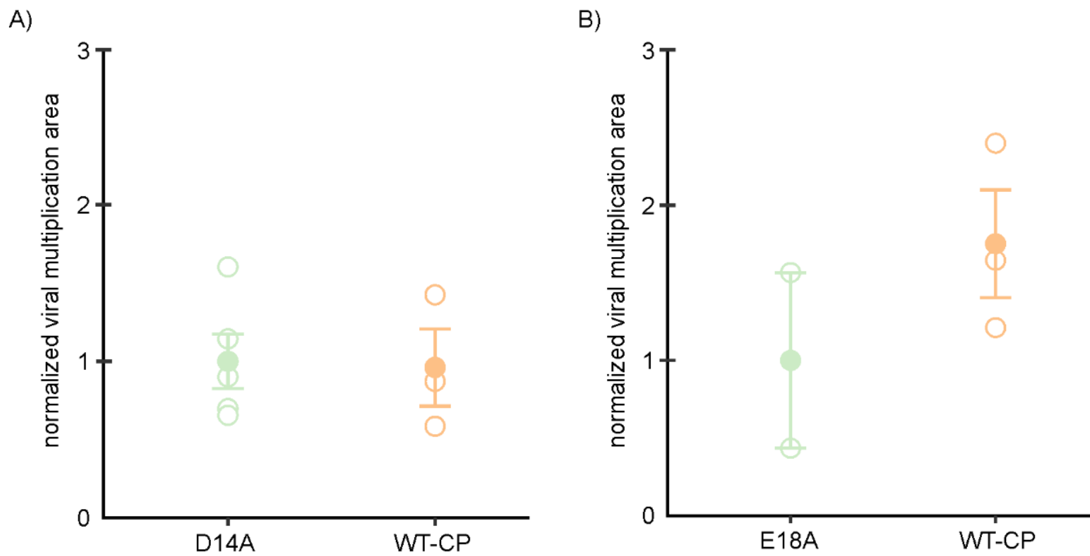

148 **Fig. S7. Virus abundance D14A, E18A, WT-CP.** Quantification of virus abundance in the upper
149 leaves of bombarded *N. clevelandii* expressed as total count per mutant for D14A mutant 7 dpb
150 with exposure time 50s (A) and (B) for E18A mutant 7 dpb with exposure time 50 (s). Other
151 measurements settings are the same as stated in Materials and methods. Mean (represented
152 with filled dot) and standard error are shown. Individual measurements are shown as empty dots,
153 representing normalized viral multiplication area. There was no statistically significant difference
154 in normalized viral multiplication area between mutants evaluated by Welch`s t test. Raw and
155 normalized data, number of plants and results of statistical analysis are specified in dataset S10
156 and S11).

157

158

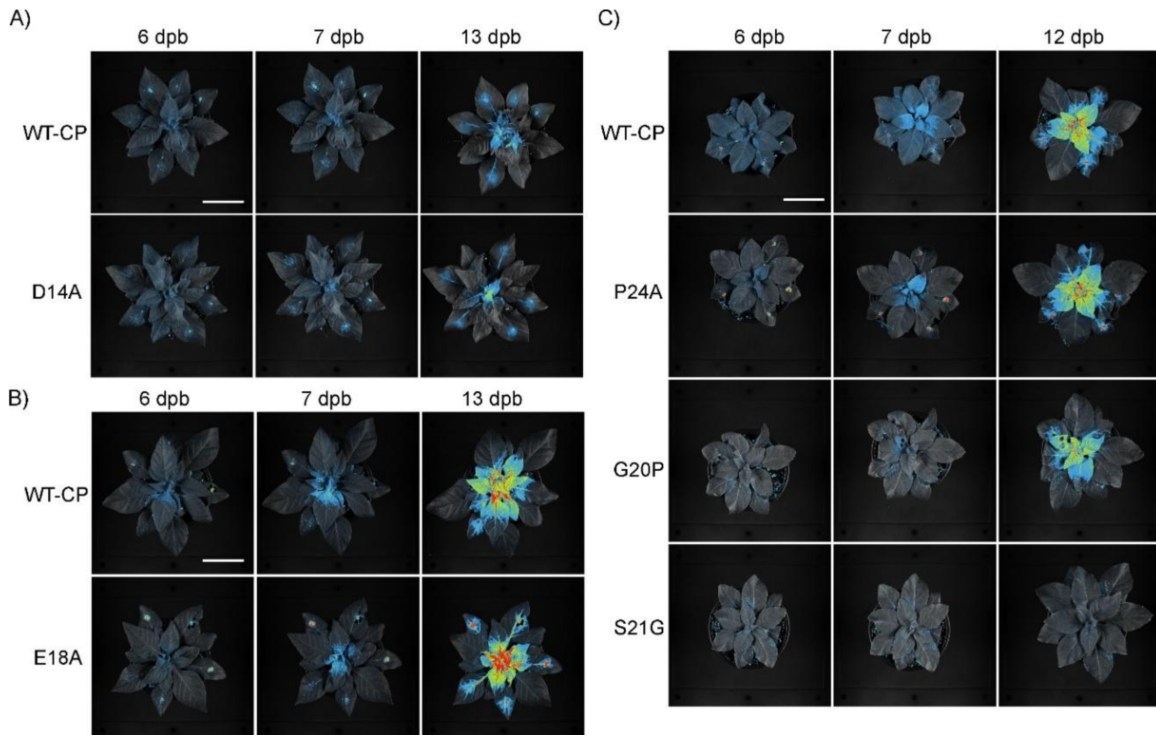

159 **Fig. S8. Point mutants systemic spread.** Spatio-temporal PVY distribution in *N. clevelandii*
160 systemic tissue using whole plant imaging system. Systemic spread of constructed point mutants
161 was followed 6 dpb, 7 dpb and 13 dpb in case of D14A (A) and E18A (B), while systemic spread
162 of P24A, G20P and S21G. (C) was followed 6 dpb, 7 dpb and 12 dpb. Note that pictures for
163 P24A, S21G and WT-CP 12 dpb are the same as in the main text (Fig. 4C). Imaging settings are
164 specified in Materials and methods. Plants were imaged with exposure time 50 s. In case of D14A
165 and WT-CP at 13 dpb, exposure time was 5 s to avoid oversaturation due to a higher signal.

166

167
168

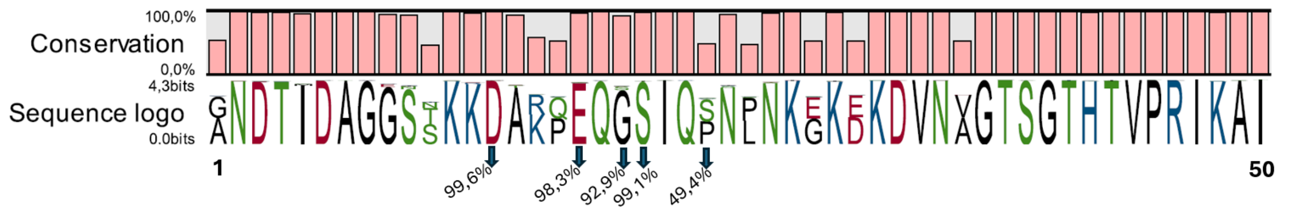

169

170 **Fig. S9 Alignment of first 50 amino acid residues from the PVY N terminal region across all**
171 **PVY isolates.** To assess the conservation of mutated amino acid residues D14A, E18A, G20P,
172 S21G and P24A, we performed multiple sequence alignment of the first 50 amino acid residues of
173 the PVY coat protein, using CLC Genomics Workbench 25 (QIAGEN, Hilden, Germany) and
174 pairwise sequence alignment. Note that for the multiple alignment analysis, only complete
175 sequences containing the first 50 amino acid residues of the PVY coat protein N terminal region
176 were included, as this region corresponds to our engineered deletion and point mutants.
177 Altogether 2112 sequences were obtained from NCBI Virus database. Sequence logo represents
178 the amino acid sequence conservation in the mutated region with arrows showing the
179 conservation percentage of each point mutated amino acid (D14A, E18A, G20P, S21G, P24A)
180 across all obtained sequences.

181

182

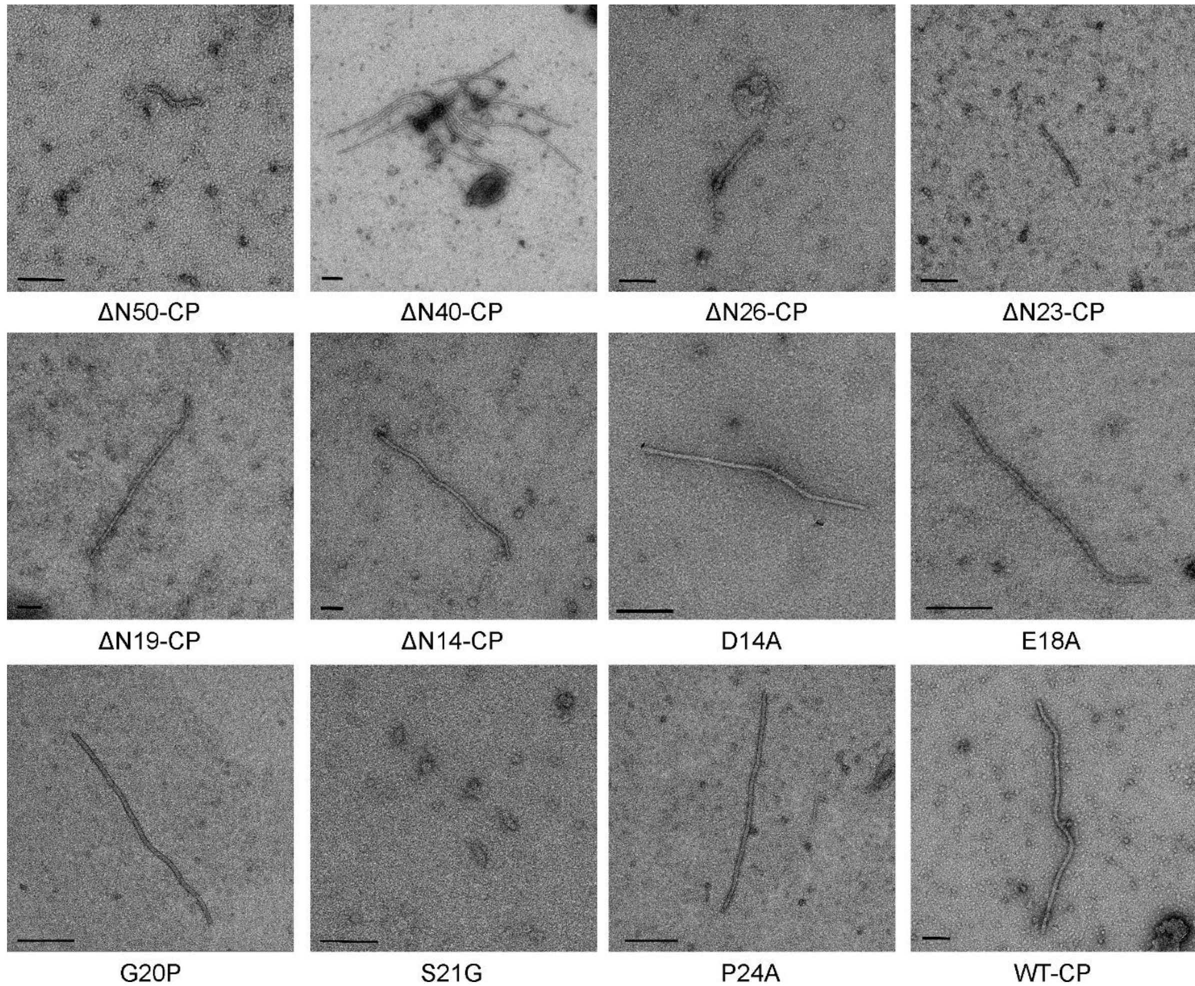

183 **Fig. S10 Transmission electron microscopy (TEM) micrographs of deletion and point**

184 **mutants.** Representative TEM micrographs of deletion mutants and point mutants. Results were

185 obtained with negative staining. Scale bars for deletion mutants and WT-CP are 100 nm and for

186 point mutations 200 nm except in case of S21G (50 nm). Additional images of the mutant viruses

187 were deposited at Zenodo (doi: 10.5281/zenodo.17643798).

188

189 **Table S1. ΔN26-CP viral limitation on single cells or cell-to-cell spread.** Number of plants

190 with viral cell-to-cell spread or viral limitation to single cells 10 and 14 dpb. Note that 5 dpb virus

191 was limited to single cells in all observed plants.

		ΔN26-CP	**WT-CP**
10 dpb	single cells	3/8	0/2
	cell-to-cell	5/8	2/2

		ΔN26-CP	**WT-CP**
14 dpb	single cells	2/3	0/2
	cell-to-cell	1/3	2/2

192

193

194 **Table S2. Replication efficiency of ΔN40-CP and S21G mutant is the same as the one of**

195 **WT-CP PVY.** To confirm that detected fluorescent signal in ΔN40-CP and S21G PVY mutants,

196 was the consequence of viral replication and not the continuous expression of viral genes from

197 the original plasmid of PVY driven by the constitutive 35S promoter, ROI (regions of interests)

198 mean intensities of individual cells in confocal microscopy images were assessed. Mean

199 intensities in selected ROIs 5 dpb for ΔN40-CP (A) and S21G (B) compared to WT-CP PVY are

200 shown. Statistical significance of differences was evaluated using Welch`s t test. Note that all

201 images were taken using the same settings (objective, zoom, gain).

A)

ΔN40-CP	WT-CP	Welch`s t test
24.4	13.8	0.6
14.0	17.1	
9.7	15.5	
13.3	9.4	
8.4	15.2	
4.8	21.6	
11.5	13.7	
8.6	15.6	
13.1	8.7	
25.7	15.9	
13.3	**14.6**	**average**

B)

S21G	WT-CP	Welch`s t test
6.8	7.1	0.2
6.8	9.4	
6.8	12.8	
6.8	**9.8**	**average**

202

203

204 **Supplemental material references**

205 1. Lukan T, Županič A, Mahkovec Povalej T, Brunkard JO, Kmetič M, Juteršek M, Baebler Š,
206 Gruden K. Chloroplast redox state changes mark cell-to-cell signaling in the
207 hypersensitive response. New Phytologist. 2023; 237(2): 548-562.
208
209 2. Stare K, Coll A, Gutiérrez-Aguirre I, Žnidarič MT, Ravnikar M, Kežar A, Kavčič L,
210 Podobnik M, Gruden K. Generation and in Planta Functional Analysis of Potato Virus Y
211 mutants. Bio Protoc. 2020; 10: e3692.
212
213 3. Kežar A, Kavčič L, Polák M, Nováček J, Gutiérrez-Aguirre I, Žnidarič MT, Coll A, Stare K,
214 Gruden K, Ravnikar M, Pahovnik D, Žagar E, Merzel F, Anderluh G, Podobnik M. 2019.
215 Structural basis for the multitasking nature of the potato virus Y coat protein. Sci Adv
216 5:eaaw3808. https://doi.org/10.1126/sciadv.aaw3808.
217
218 4. Kogovšek P, Gow L, Pompe-Novak M, Gruden K, Foster GD, Boonham N, Ravnikar M.
219 2008. Single-step RT real-time PCR for sensitive detection and discrimination of Potato
220 virus Y isolates. J Virol Methods 149:1–11. https://doi.org/10.1016/j.jviromet.2008.01.025.
221
222 5. Weller SA, Elphinstone JG, Smith NC, Boonham N, Stead DE. 2000. Detection of
223 Ralstonia solanacearum strains with a quantitative, multiplex, real-time, fluorogenic PCR
224 (TaqMan) assay. Appl Environ Microbiol 66:2853–2858.
225 https://doi.org/10.1128/AEM.66.7.2853-2858.2000

226

227